

Published in final edited form as:

Cytometry A. 2013 March ; 83(3): 306–315. doi:10.1002/cyto.a.22251.

Quantifying Spillover Spreading for Comparing Instrument Performance and Aiding in Multicolor Panel Design

Richard Nguyen¹, Stephen Perfetto¹, Yolanda D. Mahnke², Pratip Chattopadhyay², and Mario Roederer^{1,2,*}

¹Flow Cytometry Core, Vaccine Research Center, NIAID, NIH, Bethesda, MD

²ImmunoTechnology Section, Vaccine Research Center, NIAID, NIH, Bethesda, MD

Abstract

Background—After compensation, the measurement errors arising from multiple fluorescences spilling into each detector become evident by the spreading of nominally negative distributions. Depending on the instrument configuration and performance, and reagents used, this “spillover spreading” affects sensitivity in any given parameter. The degree of spillover spreading had been predicted theoretically to increase with measurement error, i.e., by the square root of fluorescence intensity, as well as directly related to the spectral overlap matrix coefficients.

Methods—We devised a metric to quantify spillover spreading between any pair of detectors. This metric is intrinsic, as it is independent of fluorescence intensity. The combination of all such values for one instrument can be represented as a spillover spreading matrix (SSM). Single-stained controls were used to determine the SSM on multiple instruments over time, and under various conditions of signal quality.

Results—SSM values reveal fluorescence spectrum interactions that can limit the sensitivity of a reagent in the presence of brightly-stained cells on a different color. The SSM was found to be highly reproducible; its non-trivial values show a CV of under 30% across a 2-month time frame. In addition, the SSM is comparable between similarly-configured instruments; instrument-specific differences in the SSM reveal underperforming detectors.

Conclusion—Quantifying and monitoring the SSM can be a useful tool in instrument quality control to ensure consistent sensitivity and performance. In addition, the SSM is a key element for predicting multicolor immunofluorescence panels, which will aid in the optimization and development of new panels. We propose that the SSM is a critical component of QA/QC in evaluation of flow cytometer performance.

Keywords

Compensation; Quality control; Sensitivity; Immunophenotyping

Introduction

A major impact of fluorescence spillover (which occurs when fluorescent probes emit light into multiple detectors) is a reduction in sensitivity (defined as the lowest signal detectable above all sources of background). The more signal from dyes with fluorescences that spill into a detector, the more the sensitivity in that detector will be diminished. In current instruments, a large source of error is the Poisson error associated with photon detection

* Address correspondence to: Mario Roederer, Vaccine Research Center, NIH, 40 Convent Dr., Room 5509, Bethesda, MD 20892-3015, Phone: 301-594-8491, Roederer@nih.gov.

(“counting error”). This error is proportional to square-root of the intensity of the signal; this leads to a non-linear (but straight-lined on a log-log plot) “spreading” of properly compensated data (1). We hypothesized that quantifying the degree of spillover spreading between every pair of measurements will be valuable for comparing instruments (2) and for guiding immunophenotyping panel design (3–5).

Here we derive an intrinsic measure of spillover spreading. The aggregation of all spillover spreading values together in a matrix is termed the spillover spreading matrix (SSM). Compared to the compensation/spectral overlap matrix¹, the SSM provides independent information about measurement performance. As we show here, the SSM is a useful indicator of instrument performance, and can be used to evaluate a single instrument over time, as well as compare different instruments. Individual SSM values perform as predicted by theory; i.e., they reflect the Poisson-based error in fluorescence quantification.

In addition, the SSM is critical information for predicting immunofluorescence panel performance. As the number of available probes and detectors continues to increase, the logistic demands on optimized panel development become too high to guarantee success by empirical methods. In the coming years, panel optimization must be guided by predictive algorithms that rely on information about reagent performance as well as instrument performance; the SSM informs about the latter in the context of any given set of reagents. To that end, we show that the SSM is a reproducible, reliable, and informative measure of instrument performance for multicolor immunophenotyping assays.

Materials and Methods

Peripheral Blood Mononuclear Cells (PBMCs) or “compensation beads” (Becton Dickinson, San Jose, CA) were stained using a variety of commercial or in-house conjugated reagents. Standard staining procedures were performed: cells or beads were stained with reagents in R10 (RPMI-1640, 10% FBS (GIBCO, Grand Island, NY), and 0.02% azide (Sigma, St. Louis, MO)) for 20 min. Cells or beads were washed twice ($400 \times g$ for 3 min) and fixed by resuspending in 0.5% formalin (Tousinis, Rockville, MD). Six cytometers, with nearly identical optical configurations, were used (5 LSR II-SORPs and an Aria II SORP, Becton Dickinson, San Jose, CA). Data analysis was done using FlowJo version 9.5 (Tree Star Inc., Ashland, OR) and JMP version 10 (SAS Institute, Cary, NC).

Results

Derivation of an intrinsic measure of spillover spreading

After compensation, the distribution of fluorescence in the spillover parameter, for a sample having a single, uniform fluorescence intensity, will have variance contributions from the intrinsic background, BV (a combination of electronic noise, light background, and autofluorescence), plus the variance from spillover-spreading, SV , arising from the added measurement error when other fluorochromes emit light in the same detector due to spectral overlap. The spillover variance SV can become the dominant source of variance and becomes particularly evident following compensation. Supplementary Figure 1 illustrates this, by graphing the theoretical distributions of samples, either compensated or uncompensated. Understanding the properties of the spillover variance can help with instrument QA/QC as well as multicolor panel design and optimization.

¹Compensation is algorithmically computed using a “compensation matrix”, which is the matrix inversion of the “spectral overlap matrix.” The latter is comprised of spillover values (e.g. “15% spillover from FITC into PE”) and is often (and incorrectly) called a compensation matrix. While having distinct values, the compensation and spectral overlap matrices are uniquely defined by each other. For clarity, we refer to “compensation/spectral overlap” matrix when either is applicable.

Variances are additive, so the total sample variance $T_V = B_V + S_V$. B_V can be measured using a reference (unstained) sample, for which S_V is zero (and thus $B_V = T_V$). These quantities can be determined for any given spillover fluorescence parameter “C,” using the standard deviation of the measurement in C from a stained sample “S” ($^S\sigma_C$) and unstained reference “R” ($^R\sigma_C$), and noting that variance is the square of the standard deviation. We thus define the spillover spreading (SS) value, $\Delta\sigma_C$, as the incremental standard deviation arising from spectral overlap, and calculate it as following:

$$\Delta\sigma_C = \sqrt{{}^S\sigma_C^2 - {}^R\sigma_C^2} \quad \text{Eq. 1}$$

A robust estimate of the standard deviation of a fluorescence distribution can be made from quantifying two percentiles within the distribution. In a normal (Gaussian) distribution, the standard deviation is approximately the difference between the 33th and 67th percentiles (i.e., the width of the central 34.1%). However, after compensation, in the spillover parameter, the lower percentile is often below zero and, on certain instruments, can be subject to aberrations in signal processing. A more robust estimate of the relevant width of the distribution in flow cytometry data is the difference between the 50th (median) and 84th percentiles (also nominally 1 standard deviation for a normal distribution). For purposes of this manuscript, the n^{th} percentile of fluorescence parameter “C” for a stained sample “S” or reference sample “R” is denoted as $^S F_C^n$ and $^R F_C^n$, respectively. Thus, for the reference (and similarly for the stained sample):

$$^R\sigma_C = {}^R F_C^{84} - {}^R F_C^{50} \quad \text{Eq. 2}$$

$\Delta\sigma_C$ (Eq. 1) was predicted to increase by the square root of the difference (between the sample and reference) in the primary fluorescence parameter intensity, ΔF_P (1). ΔF_P is calculated as the difference in median fluorescences of the two samples:

$$\Delta F_P = {}^S F_P^{50} - {}^R F_P^{50} \quad \text{Eq. 3}$$

Figure 1A–C illustrates an example calculation of these values based on experimental data.

We experimentally confirmed the predicted square-root relationship between fluorescence and spillover spreading. Compensation beads were stained with two-fold dilutions of antibody to achieve a range in fluorescence intensity (Fig 1D). For each collection, the values of $\Delta\sigma_C$ and ΔF_P were calculated as per Eq. 1–3, and plotted for two different spillover pairs (Fig 1E, F).

This relationship allows the definition of an intrinsic spillover spread value between a primary detector “P” and spillover parameter “C”:

$$SS_C^P = \frac{\Delta\sigma_C}{\sqrt{\Delta F_P}} \quad \text{Eq. 4}$$

It is intrinsic in sense that the value should be the same no matter how bright the reference sample is, and therefore should be a property of the instrument, independent of experimental conditions.

Computing this value for every pair of detectors results in a matrix of values, which we term the “Spillover Spreading Matrix” (SSM). Each column in this matrix corresponds to a detector, and each row corresponds to a fluorochrome. Every off-diagonal element is the intrinsic SS value that indicates how much error is contributed to a detector by any given fluorochrome.

The relationship between the SS value and the spillover coefficients and detector efficiency can be defined explicitly. This derivation is shown in the Appendix, as Eq. 9.

Determining the Spillover Spreading Matrix

The SSM is computed from single-stained samples as well as unstained reference samples following compensation (an appropriate set of samples would be the compensation controls themselves). Using Eqs. 1–4 (as exemplified in Fig 1A–C), the entire SSM is computed. The diagonal elements of this matrix have no meaning and are left blank. In theory, like the spectral overlap/compensation matrix, the SSM should not depend on the types of samples (e.g., beads or cells) nor how bright the samples are; it should depend only on the instrument configuration and the particular fluorochromes used.

To test this experimentally, we stained compensation beads or PBMC with 16 different fluorescent monoclonal antibodies in a single experiment. Each set of controls was subject to standard compensation matrix creation; then, from the compensated parameters, the SSM was computed. As shown in Fig 2A, the SSM was similar whether the computation was performed on beads or cells. Fig 2B illustrates the spillover spreading between one pair of detectors (specifically, Cy5PE into the Cy5.5PE detector, G710). This pair has one of the largest SS values in the matrix (as shown in the heatmaps with a magenta-colored square representing the value 13.4). The concordance of the bead-based SSM and the cell-based SSM confirms that the SSM computation is not sample-dependent, as long as the stained samples are bright enough to reveal spillover spreading. Like the compensation/spectral overlap matrix, the SSM will be accurate for any fluorescence signals at or below those used to compute it.

The utility of any metric that might be used to analyze instrument performance or aid in panel design depends on its consistency over time. Importantly, comparing SSMs across experiments is most meaningful if calibration is performed to ensure a consistent dye-to-signal level. We achieve this by doing a calibration using multi-dye reference particles before every experiment (2).

From a 14-color immunophenotyping experiment performed 11 times over a period of two months on the same instrument, we computed the variability of the individual elements of the SSM. Suppl. Fig 2 shows the CV vs. the mean SS value (for $n = 11$ replicates) for the 182 off-diagonal SSM elements. The CV is below 25% for values greater than 0.5, showing excellent reproducibility. For SS values below 0.5, the compensation controls were not sufficiently bright to accurately estimate spillover spreading, resulting in low precision. However, it should be noted that when SS values are low, spillover spreading has minimal effect on sensitivity; thus, estimating it precisely is not important.

Spillover Spreading determines maximum sensitivity (and thus resolution of populations)

The spillover spreading is related to the magnitude of the spectral overlap between two detectors as well as the sensitivity in each detector (Appendix; Eq. 9). Thus, for any given instrument configuration (e.g., lasers, filter sets, and sensitivity calibration), differences in SSMs should be solely related to the performance of the instrument. Variation in SSM over time will reveal changes in sensitivity and thus the ability to resolve fluorescent populations in any given experiment.

To illustrate the relationship between SSM and signal-to-background, we collected four bead compensation samples (and an unstained control) on an instrument with a standard filter configuration. We then collected the same set of five samples using various neutral density (ND) filters placed in the optical path of two detectors. An ND 2.0 filter, for example, reduces the incident light (and resulting signals) 100-fold, thereby reducing the signal-to-background ratio 10-fold ($\sqrt{100}$).

As shown in the examples in Fig. 3A, the spectral overlap matrices did not change dramatically despite there being a 100-fold reduction in signal (for this case, in the V800 detector). This was a consequence of adjusting the PMT voltages with each filter set so as to achieve the same fluorescence values for the calibration particles. Furthermore, the SSM did not change with the addition of the ND2.0 filter in front of the V800 detector, except for the elements involving that detector. For example, the SS value for Cy7APC into the V800 detector increased from 2.04 to 12.7. This indicates substantially more error in the compensated V800 parameter arising from Cy7APC spillover fluorescence. Indeed, this is shown in Fig 3B, which shows an overlay of the compensated distributions of CD8 Cy7APC-stained beads in the V800 parameter.

As shown in Eq. 9 (Appendix), the SS value is related to the detector efficiency for both the primary and the spillover detector. For a case where the efficiency in the spillover detector is far worse than the other (i.e., $U_C \gg U_P$), the SS value should be roughly inversely proportional to the square root of the signal-to-noise ratio in that detector. We confirmed this approximate relationship, as shown in Fig 3C. Notably, the SS value for Cy7APC into the QD800 detector (V800) is about 30-fold greater than for FITC into the PE detector (G560). This is expected, since the absolute number of photoelectrons resulting from FITC fluorescence on a cytometer is far greater, leading to much more precise measurements (i.e., $U_{QD800} \gg U_{PE}$) – although direct comparison should also take into account the spillover coefficients (eq. 9). Thus, the predicted relationship between SS values and signal-to-noise holds true across a large dynamic range.

Finally, the relationship between SS value and altered sensitivity in the primary detector is also revealed by these data. Specifically, adding an ND2.0 filter to the V800 channel increased the SSM element from R780 into QD800 from 1.28 to 4.31 – a direct consequence of U_{QD800} being increased by a factor of 100 leading to an increase in the SS value (Eq. 9).

Using the SSM to analyze instrument performance

As shown in Fig 3, with proper calibration, the absolute magnitudes of the compensation matrix elements are not sensitive to measurement noise (specifically, their precision is related to noise, but their accuracy and magnitude are independent of noise). Often, instrument performance over time is followed by tracking PMT voltages (2); increasing voltage over time can indicate degrading performance of a PMT, laser, optics, or alignment. But because each PMT has a unique transfer function, PMT voltages are not reliable for comparison of performance between instruments. By reflecting signal-to-background for consistently-calibrated instruments, the SSM may be a robust comparator of performance.

To investigate this, we computed a full 18×18 SSM on five nearly-identically configured LSR II instruments. All instruments were calibrated to the same sensitivity for any given parameter (e.g., the same target fluorescence intensity value was used for B515 (FITC) for all instruments). Interpretation of differences in SSM must take into account the dependence of SS values on spillover coefficients (eq. 9) – i.e., SS values are directly comparable only when the spillover is reasonably similar.

Figure 4A compares the SSM for two instruments. Inspection of these matrices leads to a number of interpretations: (1) the B515 (FITC) and V450 (PacBlue) parameters receive virtually no SS noise from any other parameter – indicating that measurements from these two parameters will not suffer any loss of sensitivity on these instruments, no matter how complex an immunophenotyping panel is; (2) The B710 (Cy5.5PerCP), G710 (Cy5.5PE or Ax700PE) and V705 (QD705) parameters have large error contributions from a number of fluorochromes – indicating that measurements from these parameters will suffer the most in a variety of immunophenotyping panels on our instruments; (3) PacBlue and FITC contribute relatively little noise to any other parameter, making them ideal choices for reagents detecting highly-expressed analytes. (Other considerations remain, however – such as PacBlue being relatively weakly fluorescent and not well-suited for detecting low-expressed analytes).

In Fig 4B, the SSM for all five instruments is shown, as well as each instrument's deviation from the average (individual SS values are compared in Supplemental Figure 3). Overall, the patterns are consistent; however, differences between instruments are easily identified. Most apparent is the far poorer performance of the B710 parameter on LSR-E, contributing to much more spreading in measurements from that parameter as well as any parameter into which Cy5.5PerCP fluorescence spills. Small differences in other instruments reveal potential problems in electronics, filters, or alignment that may be addressed to improve overall performance and attain equivalence.

Using the SSM to guide multicolor immunophenotyping panel design

Another practical application of the SSM is to aid design of multicolor panels, a laborious and expensive process (3,4). An example of the utility of the SSM for this process is shown in Fig. 5, using data from a recent "OMIP" (6). A comparison of three different anti-CD45RA conjugates shows the enormous impact of spillover spreading on the sensitivity for CD25 detection amongst CD45RA⁺ cells (a vast majority of which do not express CD25). As is evident by the staining examples, the use of a QD655 conjugate of CD45RA reduces the sensitivity in the G660 (Cy5PE) detector dramatically – something that could be predicted by noting that the corresponding SS value is 3–5-fold higher than for the other conjugates. For probes requiring the greatest sensitivity (e.g., CD25), optimization of the panel would include selecting fluorochromes for highly-expressed reagents (e.g. CD45RA) exhibiting low SS values into the CD25 detector.

Discussion

Spillover spreading has a significant impact on the quality of multicolor immunofluorescence phenotyping experiments. Because of fluorescence spillover, the error in measuring multiple fluorescences is propagated (under both linear and nonlinear influence of the spillover coefficient) into each output value. Thus, the more fluorescence spillovers that need to be corrected, the more variance is introduced into the final measurement. It should be stressed that compensation itself does not introduce this error; the error is there at the time of measurement and compensation simply makes it visually evident (1).

Routine determination of spillover spreading can be performed by computing the SS values between all pairs of detectors, and displaying the results in a matrix form (termed the spillover spreading matrix, or SSM). Inspection of the SSM quickly reveals which fluorescence conjugates have the greatest impact on sensitivity in any given detector. This is valuable for the process of optimizing multicolor immunophenotyping panels, in which spreading must be minimized for critical measurements. One resulting strategy is to put antigens that are mutually exclusively expressed (e.g., CD3 and CD19) on fluorescence pairs with the highest SS value, since spreading is unlikely to impact resolution of these markers.

As defined in this manuscript, the SSM is intrinsic (i.e., does not depend on the brightness of a measurement). The SSM shares this property with the spectral overlap/compensation matrix (7). Notably, for both the spectral overlap matrix and the SSM, the ability to accurately determine the matrix values does depend on the intensity of the controls: in general, the SS values are valid for measurements that are at or less bright than the controls used to compute it. In addition, the SSM depends on the calibration settings used (since the SS value includes units of the fluorescence measurement). Thus, comparison of different SSM should be done after ensuring uniform sensitivity calibration, achieved by having constant target measurement values (not constant PMT voltages) during instrument set up (2). Importantly, this means that to compare SSM between instruments, the measurement scale may first have to be normalized (i.e., to have similar measurement values for a reference sample on all fluorescence measurements).

The SSM depends the fluorochromes used. Thus, comparing the SSM on an instrument for two different fluorochromes measured on the same detector can help determine which might be a better reagent in a given multicolor panel, by revealing which leads to less spillover-spreading and thereby impacts other detectors to a smaller extent. Similarly, the SSM can be used to identify the optimal instrument configuration for an immunofluorescence experiment (i.e., that configuration of filters and lasers which minimizes the SSM for the relevant detectors).

Finally, The SSM can also be used to monitor instrument performance over time, providing a sensitive indicator of when alignment is poor, a laser is failing, or other optical issues have arisen. And, as we show in Figure 4, the SSM is a valuable tool for comparing nominally-identical instruments, revealing which detectors may require optimization.

Currently, comparing SSMs (between instruments or over time) is relatively arduous – these matrices encompass many values. The patterns from the heatmaps may not reveal important but smaller changes indicative of a problem. It may be possible to generate a summary “score” representing the entire matrix (perhaps, by summing all non-trivial SS values together) and monitoring this score for change. Confirming this will require an understanding of how much variation in SS values is acceptable or normal.

The absolute magnitude of any SS value does not have an easily-defined meaning. However, the relative magnitudes are comparable. A 10-fold increase in the SS value indicates that, for the same fluorescence intensity, there will be a 10-fold greater standard deviation in the spillover parameter measurements (and thus a 1-log greater spread of the data). Equivalently, a 10-fold increase in SS value means that the same degree of spreading in the spillover parameter measurements is achieved at 100-fold lower fluorescence in the primary parameter.

The SSM is a critical path towards automated multicolor panel optimization. When creating panels that include 6 or more colors, an exhaustive search for the optimal combination of reagents and colors becomes impossible to do experimentally. However, much of this work could be done *in silico*, by predicting reagent performance in a multicolor panel. Doing so requires knowledge of how that reagent performs by itself, as well as the SSM for a given instrument configuration (note that the spectral overlap/compensation matrix is not needed). This information is sufficient to predict performance. Theoretically, a database of individual reagent performance information derived experimentally together with a given instrument’s SSM should be enough to determine a small set of predicted optimal panels that can then be verified experimentally.

In summary, we show here the value of the Spillover Spreading Matrix for optimizing instrument performance, panel performance, and providing quality control data. The information provided by the SSM is unique and far more informative than other measures.

Supplementary Material

Refer to Web version on PubMed Central for supplementary material.

Acknowledgments

We are grateful to a reviewer who provided valuable advice and derived the relationship of SS to detector efficiency and spillover coefficients as shown in Appendix 1. We thank Dr. Joanne Yu and Margaret Beddall for manufacturing and qualifying custom conjugates used in our research, Dr. Mike Eller for collection of reproducibility data, and members of the ImmunoTechnology Section for discussions and advice. This work was supported by the Intramural Research Program of the National Institute for Allergy and Infectious Diseases of the National Institutes of Health.

Appendix

Dependence on Detector Efficiency and Spillover Coefficients

An exact relationship between the SS value and the spillover coefficients used to calculate compensation can be defined. Define the spillover coefficient (sometimes referred to as the “compensation” percentage) between the primary detector P and the spillover detector C as X_C^P . Thus, the amount of signal in the spillover detector from the primary dye measured in P is:

$$\Delta F_C = X_C^P \times \Delta F_P \quad \text{Eq. 5}$$

Further define U_C as a constant of proportionality between the signal in parameter C and the Poisson event level (i.e., the photoelectron count for the event); thus, divide eq. 5 by U_C to express the signal in Poisson units; this constant is related to detector efficiency. Based on Poisson statistics, the variance is equal to the mean of the measurement, but in Poisson units squared; thus, the variance in the spillover channel contributed by the spillover itself (as defined in Eq. 5) is shown in Eq. 6 (for Eqs. 6–9, results are all expressed in measurement units):

$$V_C^S = \frac{X_C^P \times \Delta F_P}{U_C} \times U_C^2 = X_C^P \times \Delta F_P \times U_C \quad \text{Eq. 6}$$

The signal measurement in the primary detector has its own uncertainty based on its Poisson

value of $\frac{\Delta F_P}{U_P}$; i.e. its standard deviation is:

$$\sigma_P^S = \sqrt{\frac{\Delta F_P}{U_P} \times U_P^2} = \sqrt{\Delta F_P \times U_P} \quad \text{Eq. 7}$$

The uncertainty specified in Eq. 7 also propagates to the compensation channel proportionally to the spillover coefficient X_C^P . The variance contributed is the square of this, or

$$V_p^S = \left[X_c^P \times \sqrt{\Delta F_p \times U_p} \right]^2 = \Delta F_p \times U_p \times X_c^{P^2} \quad \text{Eq. 8}$$

Finally, the spillover spreading matrix element (shown in Eq. 4) can be also written as the sum of the two variances in Eq. 6 and Eq. 8:

$$SS_c^P = \frac{\Delta \sigma_c}{\sqrt{\Delta F_p}} = \sqrt{U_c \times X_c^P + U_p \times X_c^{P^2}} \quad \text{Eq. 9}$$

The net result of this is to show the dependence of the spillover spreading matrix element on the spillover coefficient (“compensation percentage”), and, importantly, the detector efficiencies. Notably, the SS value is affected differently by changes in the gains or efficiencies of the primary and spillover detectors.

References

1. Roederer M. Spectral compensation for flow cytometry: visualization artifacts, limitations, and caveats. *Cytometry*. 2001; 45(3):194–205. [PubMed: 11746088]
2. Perfetto SP, Ambrozak D, Nguyen R, Chattopadhyay P, Roederer M. Quality assurance for polychromatic flow cytometry. *Nat Protoc*. 2006; 1(3):1522–30. [PubMed: 17406444]
3. Baumgarth N, Roederer M. A practical approach to multicolor flow cytometry for immunophenotyping. *J Immunol Methods*. 2000; 243(1–2):77–97. [PubMed: 10986408]
4. Mahnke YD, Roederer M. Optimizing a multicolor immunophenotyping assay. *Clin Lab Med*. 2007; 27(3):469–485. v. [PubMed: 17658403]
5. Mahnke Y, Chattopadhyay P, Roederer M. Publication of optimized multicolor immunofluorescence panels. *Cytometry A*. 2010; 77A(9):814–818. [PubMed: 20722004]
6. Mahnke YD, Beddall MH, Roederer M. OMIP-015: Human regulatory and activated T-cells without intracellular staining. *Cytometry A*. 2012 in press.
7. Roederer M. Compensation is not dependent on signal intensity or on number of parameters. *Cytometry*. 2001; 46(6):357–359. [PubMed: 11754206]

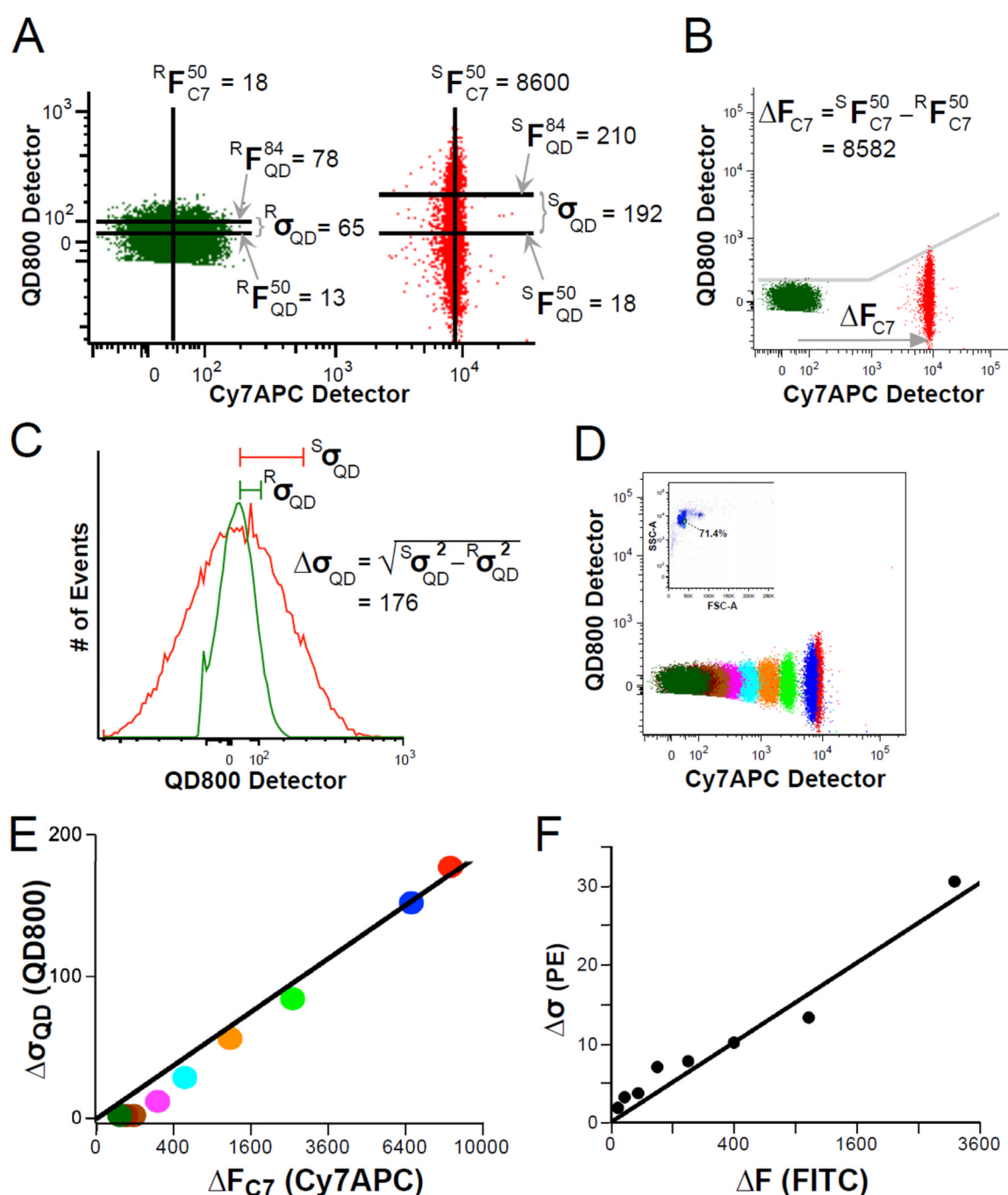


Figure 1. Computation of spillover spreading and relationship to fluorescence intensity
 (A) Compensation beads were labeled to saturation with Cy7APC CD8 (red, “sample”) or left unstained (green, “reference”); data shown are compensated for Cy7APC spillover into the QD800 detector. Lines indicate the approximate locations of various fluorescence measures used in computing spillover spreading. (B) ΔF_{C7} is the difference in median fluorescence of the reference and sample in the primary parameter (Cy7APC, on the R780 detector). The spillover spreading (indicated by the grey line) theoretically increases with the square root of fluorescence once it exceeds background fluorescence; this relationship is a straight line with a slope of $\frac{1}{2}$ on a log-log plot (see also Supplemental Figure 1). (C) The increased standard deviation due to spillover spreading ($\Delta \sigma_{QD}$) is computed based on the

measured variances in the spillover parameter of the reference and sample. (D) Compensation beads were incubated with 2-fold dilutions of Cy7APC CD8. The insert shows the gating for singlet beads. Compensated data are shown. (E, F) The relationship of $\Delta\sigma$ to ΔF is shown for Cy7APC into the QD800 detector V800 (E) and FITC into the PE detector G560 (F). Note that the x-axis is non-linearly scaled (by the square-root).

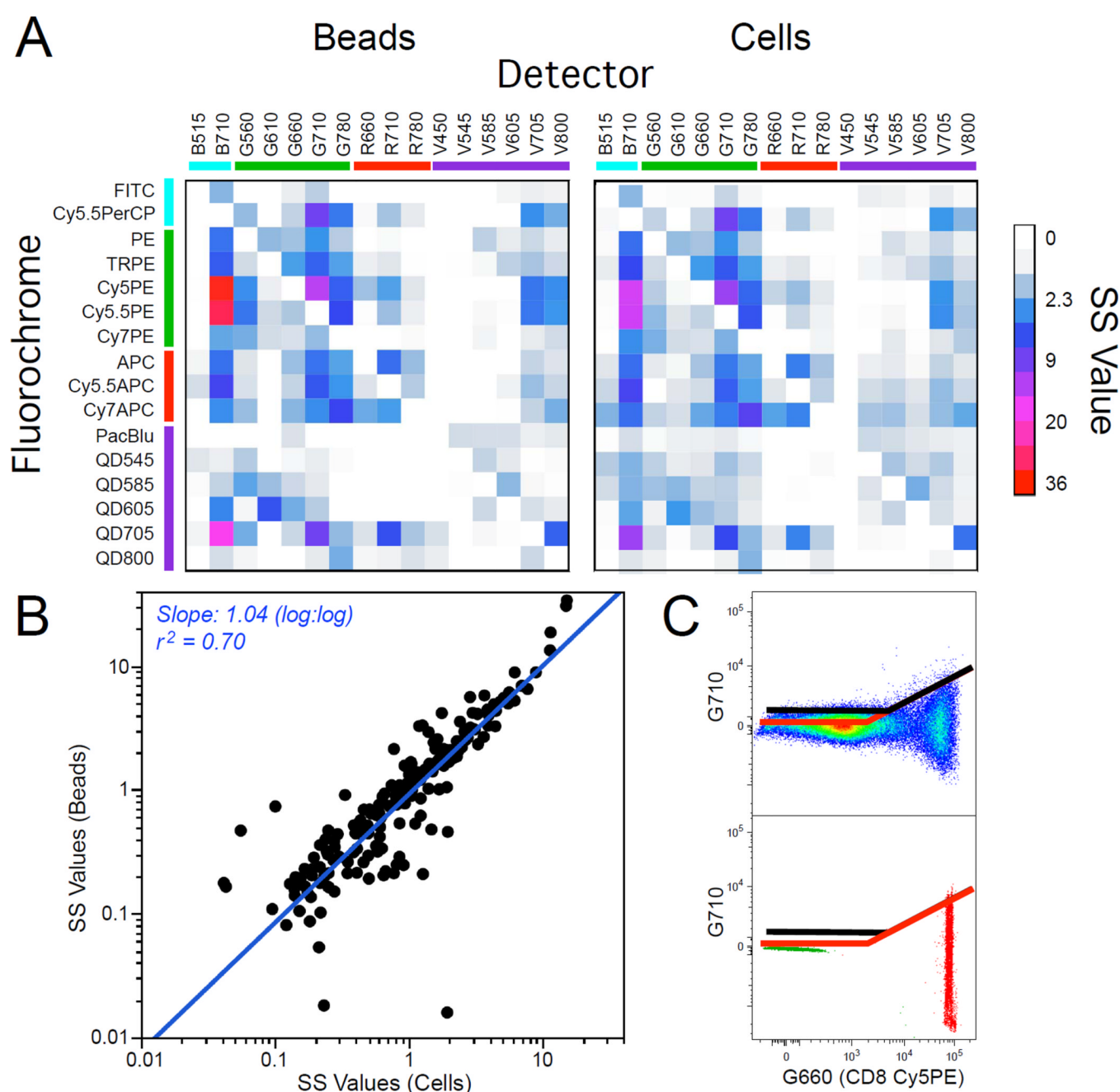


Figure 2. Spillover spreading can be computed from beads or cells

(A) Beads or PBMC were stained with 16 fluorescent conjugates and used to create respective compensation matrices. The compensated data were then used to determine the SSM for each. Each cell of the heatmap is colored according to the magnitude of the SS value. The colored bars on the left and top indicate which laser was used for detection (cyan: 488 nm; green: 532 nm; red: 632 nm; violet: 405 nm). (B) The 240 off-diagonal SS elements of the two SSMs shown in panel A are graphed against each other to demonstrate quantitative similarity. A least-squares regression on the log-transformed values was performed. Most outliers occur with SS values <1, which are less reliable and perhaps trivial (see Supplemental Figure 2). Indeed, the correlation coefficient (r^2) for SS values >1 is 0.80. (C) Cells (top) or beads (bottom) labeled with Cy5PE CD8 are shown following

compensation for the primary parameter (G660) vs. a spillover parameter (G710). The black (cells) or purple (beads) lines are a depiction of the approximate spreading for each control type; it rises only when the variance from spillover spreading exceeds that of the unstained substrate.

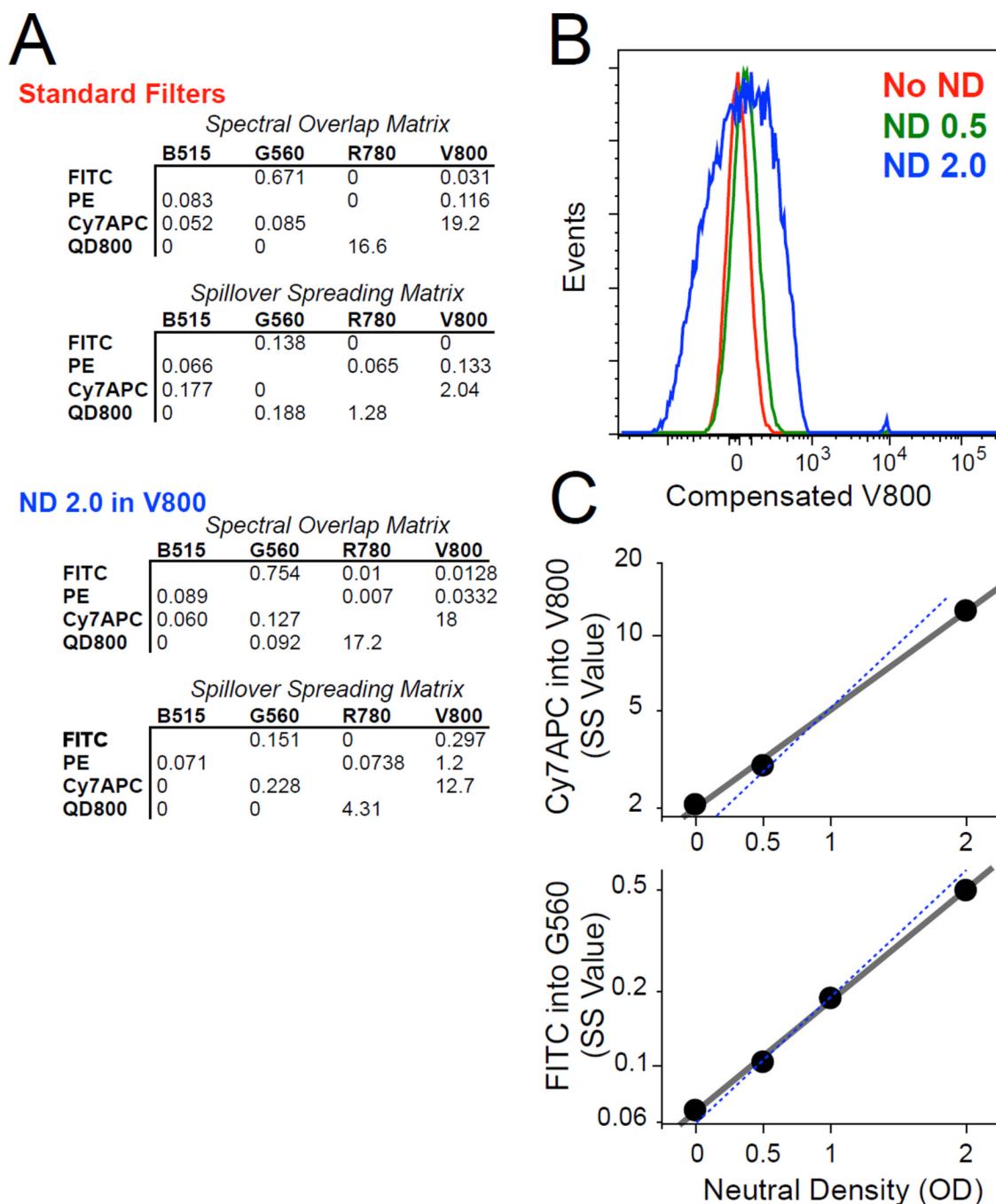


Figure 3. Spillover spreading values reflect noise contributions independently from compensation values

(A) Spectral overlap matrix and SSM for a 4-color experiment with standard filters or with an added ND2.0 (i.e., reducing signal by 100-fold) in the V800 parameter. (B) Compensated distributions of CD8 Cy7APC-stained beads in the V800 (spillover) parameter for data collected with different ND filters in the V800 detector. (C) Relationship of the spillover spreading (SS) value to the signal level for CD8 Cy7APC-stained beads in the V800 detector (top) or for FITC stained beads into the G560 (PE) detector (bottom). Note that the SS values are plotted on a log scale; ND values scale logarithmically with signal attenuation. The line is a linear least-squares fit of the log-scaled data; the blue dashed lines indicate a

theoretical relationship for which SS scales by the square-root of signal-to-noise. The deviation from this relationship is likely due to an additional linear dependence of SS on signal-to-noise (Appendix; eq. 9).

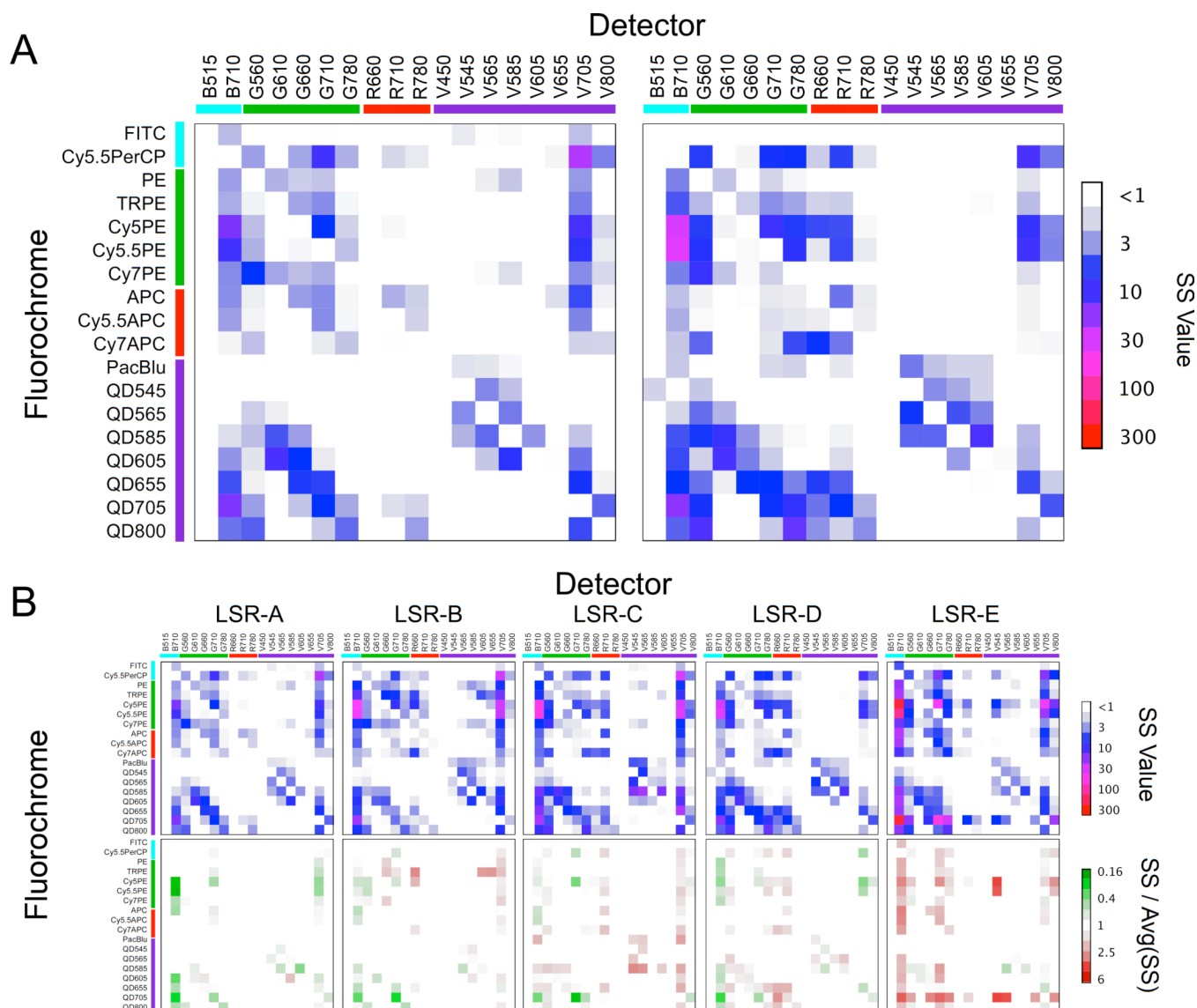


Figure 4. The spillover spreading matrix (SSM) for instrument comparison

The SSM was computed for the same stained bead samples collected on each of five nearly-identically-configured instruments. (A) A heatmap representation of the SSM is shown for two instruments (LSR-A, LSR-D). The colored bars on the left and top indicate which laser was used for detection (cyan: 488 nm; green: 532 nm; red: 632 nm; violet: 405 nm). (B) The top row show the heatmaps for all five instruments. The bottom row shows the ratio of each instruments' SS values from the average across all five (for SS values less than 0.5, the ratio was set to zero for the heatmap). Green indicates SS values smaller than average; red indicates SS values larger than average.

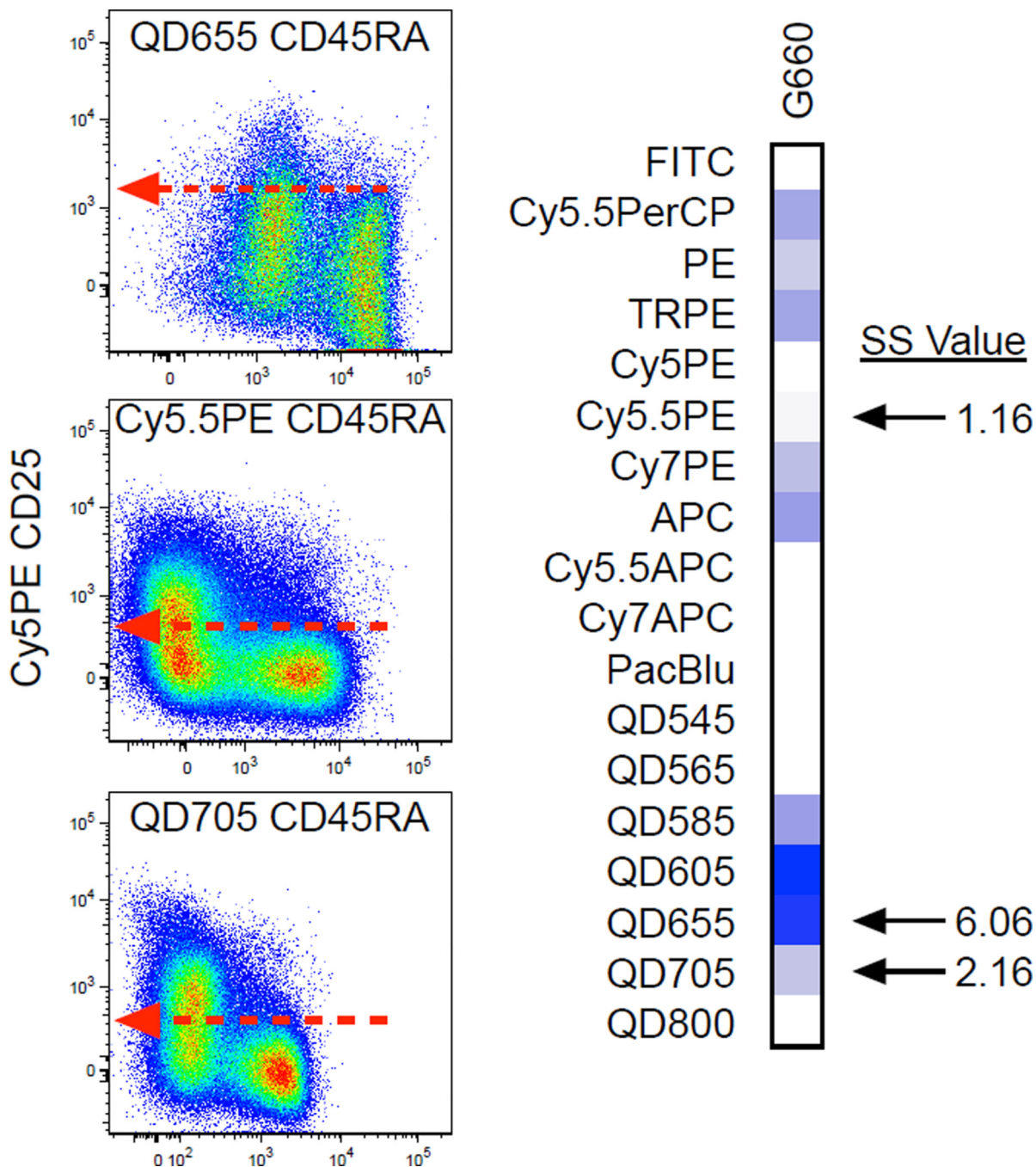


Figure 5. Multicolor immunophenotyping and the spillover spreading matrix
 (Left) Bivariate distributions of CD4⁺ T lymphocytes is shown for three different combinations of reagents, showing the expression pattern for CD25 (conjugated to Cy5PE) vs CD45RA (on three different fluorochromes) for the same PBMC sample. The degree of spillover spreading (indicated by the dashed lines) limits sensitivity for detection of CD25. Data taken from a published OMIP (6). (Right) The heatmap representation for spillover spreading into the G660 detector (for Cy5PE) on the instrument. The three values corresponding to the reagent combinations shown on the left are indicated.